Acoustically Levitated Whispering-Gallery Mode Microlasers: Supplemental document

1. DIGITAL IMAGE PROCESSING

The flowchart in Fig. S1 describes the Digital Image Processing (DIP) protocol for extracting the droplet's geometrical properties and position, developed as a set of functions written in MATLAB®. The first step acquires images with a low-cost USB microscope camera with 2 Mpx of resolution positioned in the xz-plane, see Fig. S1(a) that depicts a representative droplet picture. A region of interest (ROI) within the image is selected, then the RGB channel that provides higher contrast is isolated. In this work, we swap between red and green channels depending on the plane of capture see Fig. S1(b). A Canny algorithm [1] isolates the droplet edges providing the binary image in Fig. S1(c). The nearest contour white pixels, relative to the image edge, are detected and fed to an ellipsoidal fit algorithm based on the code given by [2]. The fitting algorithm provides semiaxis lengths and the central droplet position (Cx, Cy) depicted in Fig. S1(e).

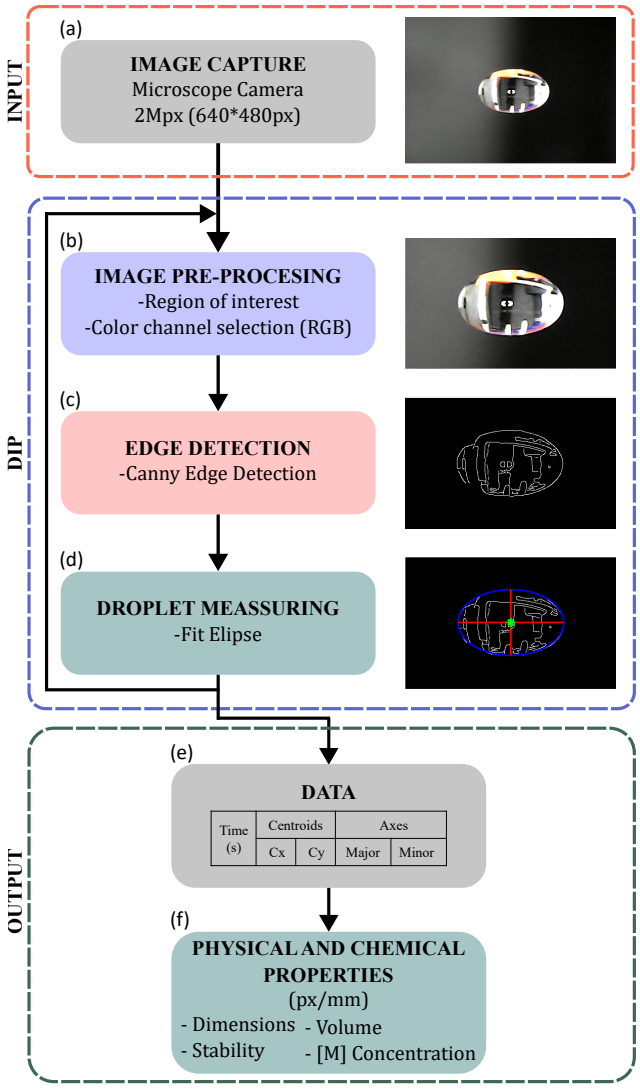

Fig. S1. Digital image processing protocol applied for the photographs processing of the levitated microdroplets.

2. DROPLET VOLUME REPRODUCIBILITY

The average volume fluctuation of levitated droplets, computed with 50 repetitions, provides a criterion for assessing experimental repeatability. Droplet volume measuring uses the DIP protocol described above, where two USB microscope cameras capture the droplet top and lateral planes. Fig. S2 shows the initial calculated volume for 50 droplets injected with a micro-pump (New Era NE-4000) with a programmed volume of 8 µl and a constant rate of 100 µl·min^{-1}. The average droplet volume fluctuation is 7.95 $\pm$1.12µl, which is a consequence of the fluids mass injection variations explained in [3–5].

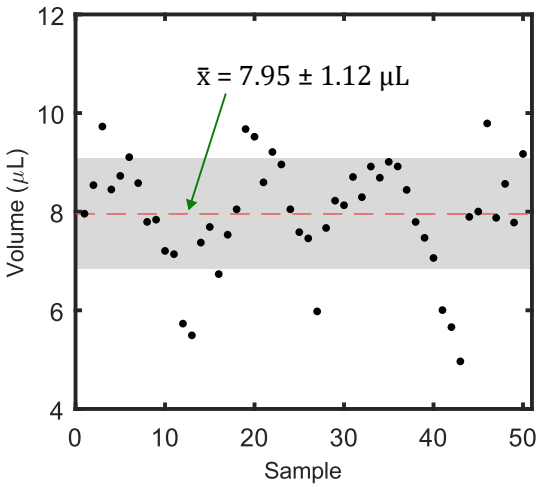

Fig. S2. Reproducibility in the volume of injected microdroplets.

In addition, to determine an optimal injection rate (µl·min^{-1}), different initial droplet volumes at different injection rates were characterized; the average droplet volume and its standard deviation for each volume/rate configuration are presented in Table S1.

Volume (µl)	Rate (µl·min^{-1})	$\bar{x}$ (µl)	σ (µl)
5	50	4.68	0.53
5	100	4.81	0.64
5	200	4.84	0.63
8	50	7.39	1.15
8	100	7.95	1.12
8	200	7.73	1.56
10	50	10.24	1.58
10	100	10.21	1.74
10	200	9.18	2.10

Table S1. The average ($\bar{x}$) and the standard deviation (σ) in terms of different droplet volumes at different injected rates.

DIP processing results indicate that smaller volume injection leads to smaller droplets, compromising the droplet evaporation time and limiting the optical lasing characterization. Conversely, volumes greater than 8 µl result in bigger droplets; due to the configuration of our levitating system, they are not the best in terms of stability.

3. DROPLET EVAPORATION FROM A TIME-LAPSE VIDEO

A time-lapse video, recorded with the lateral xy-plane USB microscope, contains all photographs processed under the DIP protocol for an experimental droplet time evolution experiment. See Visualization 1.

4. OPTICALLY EXCITED LEVITATED MICROLASER

The movie Visualization 2 gives an example of a fluorescent dye-doped levitated microdroplet.

5. ARRANGEMENT OF THE ACOUSTIC TRANSDUCERS

The array of transducers used in this work is schematically represented in the Fig. S3, each blue point represents the spatial distribution of the 36 acoustic transducers. Each cap holder has two concentric rings with transducers arranged evenly every 43.03° in the larger ring, and 21.52° in the smaller one. Both semispherical holders are separated 7 cm from their centers concerning the z-axis.

Figure S3(a) schematizes the 3D spherical formation with R = 35 mm, the xy and xz-planes are presented in Fig. S3(b) and (c), respectively. The positions for the 36 sources are calculated as follows:

$$r_\ell = (r_1 \cos\phi_i,\, r_1 \sin\phi_i, z_1), \quad \phi_i = \tfrac{\pi}{3} i, \quad \text{with } i\text{=1 to 6,} \tag{S1}$$

$$r_\ell = (r_1 \cos\phi_i,\, r_1 \sin\phi_i, 2r_s - z_1), \quad \phi_i = \tfrac{\pi}{3} i, \quad \text{with } i\text{=1 to 6,} \tag{S2}$$

$$r_\ell = (r_2 \cos\phi_i,\, r_2 \sin\phi_i, z_2), \quad \phi_i = \tfrac{\pi}{6} i, \quad \text{with } i\text{=1 to 12, and} \tag{S3}$$

$$r_\ell = (r_2 \cos\phi_i,\, r_2 \sin\phi_i, 2r_s - z_2), \quad \phi_i = \tfrac{\pi}{6} i, \quad \text{with } i\text{=1 to 12.} \tag{S4}$$

The Cartesian axis center is localized below the sphere, with radius $r_s = 35$ mm, centered in $(0, 0, 35)$.

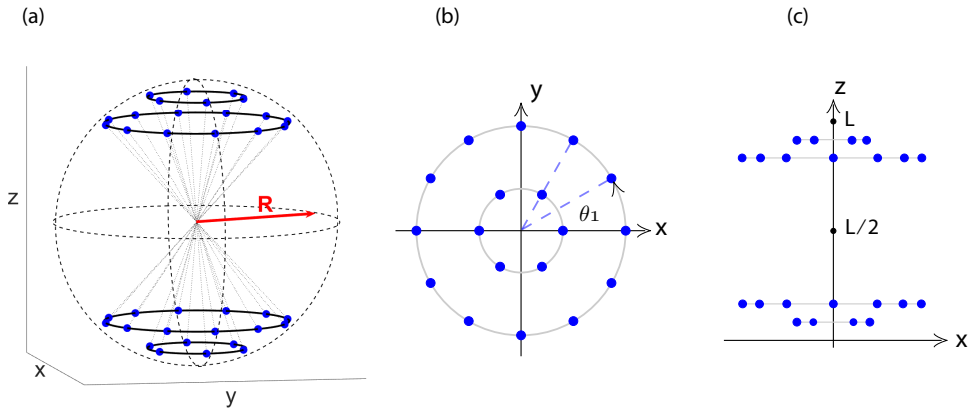

Fig. S3. Transducers arrays, visualized in (a) 3D, (b) for the xy-plane, and (c) the xz-plane.

6. OPTICAL ABSORPTION AND EMISSION OF RHODAMINE B SOLUTIONS

Optical absorption and emission spectra of 1×10^{-4}, 5×10^{-5}, 1×10^{-5}, and 5×10^{-6} M solution concentrations of Rhodamine B in distilled water. The solutions were characterized via a fluorometer (FS5, Edinburgh Instruments)[6]. Fig. S4 shows the photoluminescence (PL) spectra of solutions at different concentrations. The lowest RhB solution (5×10^{-6} M) has a peak of emission at $\sim$ 605 nm with a shoulder at $\sim$ 630 nm; the fluorescence spectra present a red shifting $\sim$ 30 nm respect their corresponding absorption spectra [34–36]. The peak of emission for the sample with the bigger concentration of 1×10^{-4} M is further red-shifted. Here, the multiple internal effects (i.e., reabsorption) modify the registered spectrum [6, 7].

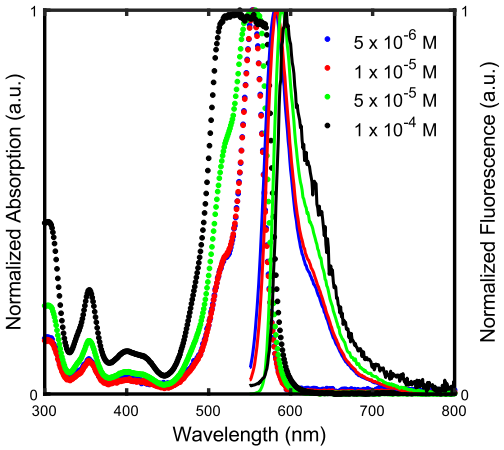

Fig. S4. Optical absorption and emission spectra for all the RhB solution under test.

7. THE CAVITY GEOMETRIC LENGTH

Taking into account that not a single periodic orbit exists inside the cavities, the spectrum's Fourier Transform (FT) helps us to identify the lasing periodic orbits. As an example, Fig. S5(a) shows the experimental emission spectrum of a levitated droplet with $5\times10^{-}6$ M at 311 nJ·cm^{-2}; Fig. S5(b) is its corresponding Fast Fourier Transform (FFT). The noisy signal observed from the complete FFT results from erratic trajectories supported inside the microcavity. Fig. S5(c) shows the histogram where the wavelength difference between consecutive peaks is summarized. By fitting a Gaussian function, a chief FSR = 0.96 nm is obtained by following the relation FSR $= \lambda_m^2/L * n_{eff}$ from where L = 3.46 mm, which agrees with the equatorial geometrical diameter of our device.

For example, by considering the highlighted green region in Fig. S5(a) where the inter-peaks distance corresponds to the previously calculated FSR, the FFT is calculated there. Fig. S5(d) displays the resulting FFT, revealing two main optical lengths (L_o). Using the relation $L_G = L_O/n_g$, with n_g as the group refractive index (approximately 1.63 for our system), we obtain L_G = 2.02$\pm$ 0.2 mm and L_G = 3.46 $\pm$ 0.2 mm. The first corresponds to a sub-orbit close to the poles, while the second corresponds to the equatorial diameter. These geometrical lengths, determined from the droplet images, are consistent with the presented results.

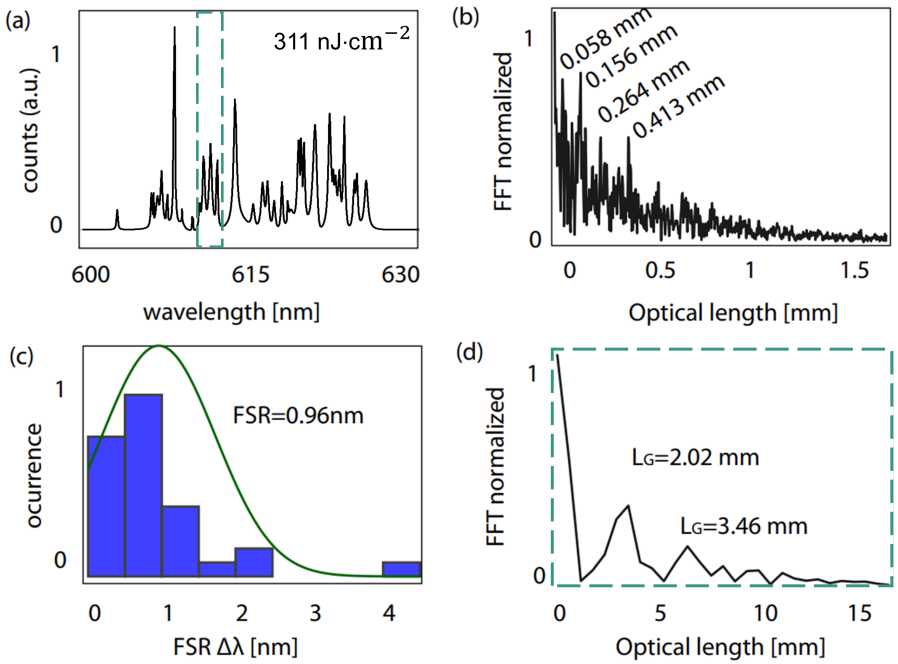

Fig. S5. (a) Lasing emission spectrum from a levitated droplet with 5×10^{-6} M, registered at 311 nJ·cm^{-2}. (b) Complete FFT, and (c) the Histogram of neighboring peak spectral separations, yielding the calculus of FSR. (d) The corresponding FFT of the highlighted section in (a).

REFERENCES

1. Rachmawan, "Canny edge detection," `https://www.mathworks.com/matlabcentral/fileexchange/46859-canny-edge-detection`.
2. O. Gal, "fit_ellipse," `https://www.mathworks.com/matlabcentral/fileexchange/3215-fit_ellipse)` (2023).
3. J. U. Álvarez-Martínez, O. M. Medina-Cázares, M. E. Soto-Alcaraz, R. Castañeda-Priego, G. Gutiérrez-Juárez, and R. Castro-Beltrán, "Microfluidic system manufacturing by direct laser writing for the generation and characterization of microdroplets," J. Micromechanics Microengineering **32**, 065001 (2022).
4. Z. Li, S. Y. Mak, A. Sauret, and H. C. Shum, "Syringe-pump-induced fluctuation in all-aqueous microfluidic system implications for flow rate accuracy," Lab on a Chip **14**, 744–749 (2014).
5. W. Zeng, I. Jacobi, D. J. Beck, S. Li, and H. A. Stone, "Characterization of syringe-pump-driven induced pressure fluctuations in elastic microchannels," Lab on a Chip **15**, 1110–1115 (2015).
6. H. Reynoso-De La Cruz, I. Rosas-Román, G. Ramos-Ortiz, B. Mendoza, E. Ortiz-Ricardo, G. Gutiérrez-Juárez, and R. Castro-Beltrán, "Studies of the transition between amplified spontaneous emission and optical lasing in ultrahigh-q polymeric micro-pedestals," Opt. Express **31**, 9018–9033 (2023).
7. S. A. Raza, S. Q. Naqvi, A. Usman, J. R. Jennings, and Y. W. Soon, "Spectroscopic study of the interaction between rhodamine b and graphene," J. Photochem. Photobiol. A: Chem. **418**, 113417 (2021).